Using Algebraic Reconstruction in Computed Tomography

Nate D. Tang
University of Canterbury
Department of Physics and Astronomy
Christchurch, New Zealand
dta37@Uclive.ac.nz

Niels de Ruiter
University of Otago
Department of Radiology
Christchurch, New Zealand
nielsde@gmail.com

J. L. Mohr
University of Otago
Department of Radiology
Christchurch, New Zealand
judy.mohr@otago.ac.nz

A. P. H. Butler
University of Otago
Department of Radiology
Christchurch Hospital, New Zealand
anthony@butler.co.nz

P. H. Butler
University of Canterbury
Department of Physics and Astronomy
Christchurch, New Zealand
phil.butler@canterbury.ac.nz

R. Aamir
University of Canterbury
Department of Physics and Astronomy
Christchurch, New Zealand
ayr13@uclive.ac.nz

ABSTRACT

Spectral Computed Tomography (spectral CT) is a newly emerging, medical imaging modality. It extends CT by acquiring multiple datasets over different x-ray energy bins. As the x-ray absorption of materials is energy dependent, the energy bins together provide significantly more information about the composition of the subject.

To exploit the full potential of spectral CT, there are many new image processing challenges including reconstruction, material decomposition, and visualization.

This paper introduces the development of a unique reconstruction algorithm which fully exploits the nature of spectral CT data. A small application called mART was developed which implements a standard Simultaneous Algebraic Reconstruction Technique (SART). mART will form the basis for future research and development.

We demonstrate that in its current form it produces reconstructions of superior quality to the commercial reconstruction package Octopus CT® which is the standard software adopted by our team. In addition, future plans for the reconstruction algorithm will be discussed.

Keywords

computed tomography, reconstruction, Octopus, ART, filtered back projection

1. INTRODUCTION

Computed Tomography (CT) is a medical imaging procedure that is fundamental to disciplines in both diagnostic and therapeutic medicine. CT scanners acquire x-ray based, radiographical images at various angles around a subject. Reconstruction algorithms then produce a volumetric image of the original subject [1].

Conventional CT imaging, while providing information at a high resolution of up to 500um spatial resolution, produces images that cannot reliably distinguish differences in soft tissue and various contrast agents used in biomedical imaging.

The Medipix All Resolution System (MARS) project aims to advance CT into the realms of spectral CT. Spectral CT measures not only x-ray intensity (measured in photon counts) but also the energy associated with the detected photons. As the linear attenuation for materials is energy dependent, the potential for material decomposition algorithms is significantly improved.

A key task leading to the success of the MARS project is the image processing of the spectral CT data. In particular, material decomposition and reconstruction algorithms have the potential to exploit the nature of spectral CT data. This can improve image quality and reduce dose requirements.

The current reconstruction software adopted by the MARS team is Octopus CT by InCT systems [2]. This is a commercial application based on filtered back projections [3]. To reconstruct data from the MARS scanner, each energy bin is reconstructed independently. While successful, it does not use the full potential of the data acquired and does not cope well with reconstructing images of low photon counts. This results in high exposure times, and large over-sampling to produce scans of sufficient quality. Neither case is ideal for future clinical use.

This paper introduces the groundwork for developing a reconstruction algorithm that meets the needs of the MARS project. The algorithm used is an algebraic reconstruction technique (ART) called SART. The basis model for ART in equation (1) is simple and flexible. In particular, it is easy to incorporate prior knowledge, constraints, and custom data structures such as the multiple values per detector element acquired by spectral CT. This makes ART a good basis for spectral reconstruction.

$$\mathbf{A}\boldsymbol{x} = \boldsymbol{b} \tag{1}$$

This paper examines images produced using our implementation of ART and compares them to equivalent images produced using the current reconstruction methods. Section

WOODSTOCK '97 El Paso, Texas USA

2 outlines the implementation of ART used. Section 3 discusses the measures used to quantify image quality. Section 4 discusses the differences seen between the two methods of reconstruction, with concluding remarks found in section 5.

2. ALGEBRAIC RECONSTRUCTION

The theory behind reconstruction algorithms was first introduced by Johann Radon in 1917 [4]. Radon's work describes the mathematical procedure for recreating a subject image from many projection images by using the inverse Radon transform.

However, the inverse Radon transform can not be solved analytically in its basic state. A solution was found by Bates and Peters in 1971 [5], by using Fourier transforms to simplify the problem. This method became known as filtered back projection. After Godfrey Hounsfield [6] popularized the CT scanner in 1972, filtered back projection quickly became the solution of choice due to its high computational efficiency.

Another common reconstruction approach is the algebraic approach which has been around since the start of CT. In fact, an algebraic solution was used by Hounsfield himself in his original work [6]. Since then, many variations of ART have arisen to improve quality, speed, and to meet the needs of new scanner technologies.

There are three common variations of ART that exist today based on iterative methods of solving equation (1). The basic method is the Kaczmarz equation [7] shown in equation (2). When referring to ART, this algorithm is usually assumed. While very effective, variations of this method arose to improve on the results.

$$\boldsymbol{x}_k = \boldsymbol{x}_{k-1} + \frac{\boldsymbol{b}_k - \boldsymbol{x}_{k-1} \cdot \mathbf{A}_i}{\mathbf{A}_i \cdot \mathbf{A}_i} \cdot \mathbf{A}_i \tag{2}$$

The first of such variations was the Simultaneous Iterative Reconstruction Technique (SIRT) proposed by Gilbert in 1972 [8]. SIRT updates the voxel values, $\boldsymbol{x}_k$ with the average of all weighted differences from all detector elements over all projection angles that contribute to the voxel. This yields results of superior quality at the cost of significantly increasing the time to convergence.

Another variation, which is a balance between standard ART and SIRT, is the Simultaneous Algebraic Reconstruction Technique (SART) proposed in 1984 by Anderson and Kak [9]. In this variation, the voxel updates are the averaged weighted differences from all detector elements in a single projection angle that contributes to a voxel. This provides a good balance between speed and quality.

A different approach is the Multiplicative Algebraic Reconstruction Technique (MART) proposed by Gordon in 1970 [10]. Most iterative algorithms adopt an additive solution. MART, as the name suggests is a multiplicative solution with a few important consequences. Firstly, the MART algorithm converges faster due to its simpler structure. Secondly, a voxel value of zero will nullify progress of the algorithm which can yield incorrect results. Lastly, MART has a tendency of magnifying noise while the additive methods tend to average noise.

Recent developments in ART have shifted away from iterative solutions in favour of compressed sensing techniques [11]. Compressed sensing techniques apply known constraints to the system to reduce the amount of data required to reconstruct a signal. This has the potential to greatly reduce dose for images of equivalent quality. The only downsides are high complexity and low computational efficiency.

2.1 Algorithm for Spectral CT Reconstruction

The ideal reconstruction algorithm for spectral CT data would be one which incorporates all the available data. For the MARS scanner, the acquired data represents the count of photons registered above a set energy threshold. Therefore, the spectrum of energies acquired ranges from the selected low threshold to the maximum energy produced, set via the x-ray voltage limit (kVp).

In spectral CT, data for all energy bins are acquired over the same field-of-view. This means that all energy bins contain the same geometrical structures. Therefore each energy bin should improve the spatial resolution of the other energy bins if processed correctly.

To meet the target goal for spectral CT reconstruction, the adopted approach is to extend an existing reconstruction algorithm. The algorithm selected for developement was SART. This is because the core ART model (equation (1)) is simple, flexible, and closely maps the physics of the scanning process. In addition, SART has proven in the past to have a good balance between quality and performance [9, 12].

The core ART model can be directly derived from the Beer Lambert Law:

$$C = C_0 e^{-\mu d}. \tag{3}$$

The Beer Lambert Law links the measured counts C to the transmission μd along a single ray from the source to a detector element. Transmission has the property that it can be divided into a sum of smaller steps, such that

$$\mu_T d_T = \sum \mu_i d_i. \tag{4}$$

This expression represents a single row of equation (1) where $\boldsymbol{b}_n = \mu_T d_T$, $\mathbf{A}_{n,i} = d_i$, and $\boldsymbol{x}_i = \mu_i$.

There are three parts to the SART solution which may be altered if necessary.

The first part is the initial value of the volume, $\boldsymbol{x}$. The closer this is to the solution, the faster convergence will be. A very simple form of spectral CT reconstruction would be to use the result from one energy bin as the starting value of another. The geometrical structures will then be present right from the start and improve performance.

The second part of the SART solution which may be altered is the geometrical model of the scanner. The values of the $\mathbf{A}$ matrix in the ART model, represents the average path length through a volume voxel which contributes to a detector element. The more accurate the scanner model, the more precise the values of the $\mathbf{A}$ matrix will be. The current implementation uses 11 geometrical transformations, including translations, offsets, rotations, and skew angles. Scanner specific metrics, such as flex and vibration, were not considered in the current model.

The third simple adjustment is the handling of dead pixels. Traditionally, dead pixels are filled in by an approximation. This process is generally referred to as inpainting. This works well for small dead regions, however, for large dead regions inpainting does more harm than good. If an object is hidden behind a dead region, then the inpainting is guaranteed to produce incorrect results.

The other option is to note that equation (1) is a large underdetermined system. This is because it is desirable to

minimize dose and hence, minimize the number of values in $\boldsymbol{b}$. If a value of $\boldsymbol{b}$ is dead, then the row corresponding to that value can simply be removed. This results in a slightly more underdetermined system which can produce better results than reconstructing from incorrect values after inpainting.

With all of the above points taken into consideration, a small application called mART was developed which implements SART. The implementation is a single threaded CPU solution aimed at producing high quality reconstructions. Once this first milestone is achieved, the algorithm can be optimized and extended for spectral CT reconstruction.

The current form of mART reconstructs data from individual chip images. This is to allow sub-pixel geometrical alignment without the blurring associated with stitching algorithms. Inpainting of dead pixels is optional where dead pixels are simply ignored if present in the data.

3. MEASURING IMAGE QUALITY

The first test for mART is to compare the output with that of Octopus CT, however the way in which image quality can be assessed are numerous. This paper employs two main methods: the assessment of the graininess of an image and the sharpness of the edges within the image.

The graininess of an image, from hence forth referred to as noise, limits the contrast sensitivity of a CT image, and hence its ability to detect features within the image itself. The noise of an image is evaluated by measuring the relative standard deviation in CT numbers over a uniform region of interest, where the CT number is the normalised unit of attenuation in Hounsfield units (HU) and is independent of the scanner. CT numbers are defined such that the CT number for air and water are -1000 HU and 0 HU respectively. Larger noise values represent more variation in CT numbers across the region of interest, and hence more graininess.

The sharpness of the edges within an image can be related to the spatial resolution, and is a measure of the ability to resolve fine detail. It can be measured from the modulation transfer function (MTF). An annulus mask is applied to an image, shown in Figure 1(a), from which the MTF can be determined by direct analysis of the edge response function. The 10% MTF value, shown in Figure 1(b), represents the number of line pairs distinguishable in a millimetre [13].

4. RESULTS AND DISCUSSION

This comparison of reconstructions from mART and Octopus CT was performed using both simulated and real data of standard phantoms. All images presented in this section are normalised to standard CT numbers.

The Shepp-Logan phantom is a standard simulated phantom used in a variety of tomographic medical imaging applications. Synthetic Shepp-Logan phantom images were simulated by MATLAB using the 3D modified Shepp-Logan algorithm. As this phantom does not specifically contain any regions of water, to determine the attenuation value of water in reconstructed images, a uniform region of the interior was selected, whereas a region of the surrounding medium was selected to determine attenuation values for air.

Figure 2 shows selected reconstructed slices of the Shepp-Logan phantom using Octopus CT and mART algorithm, when using 72, 180 and 360 x-ray projections in the reconstruction. When using 360 projections the resulting images are visibly similar, however at 72 projections Octopus CT

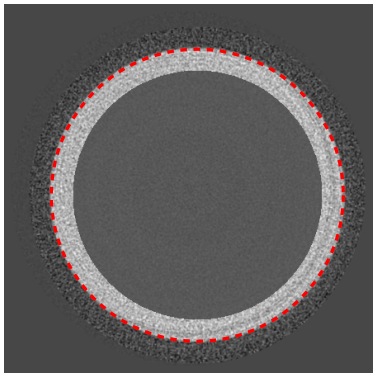

(a)

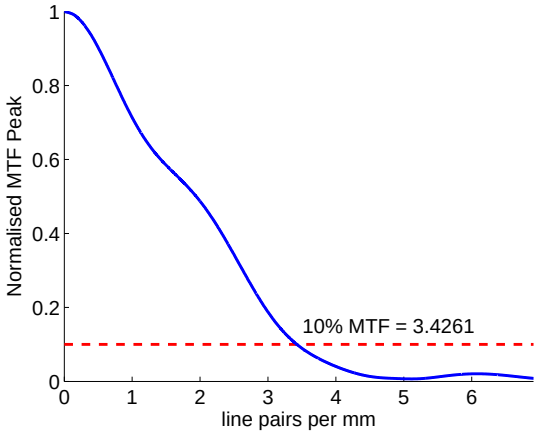

(b)

Figure 1: Spatial resolution determination. (a) An annulus mask is applied to an image, from which the MTF can be determined. (b) The 10% MTF value defines the number of line pairs distinguishable in a millimetre.

Table 1: Noise and spatial resolution values for mART reconstructions of Shepp-Logan images. 10% MTF values is in line pairs per mm.

Shepp-Logan	Noise(HU)	10% MTF
72 projections	4.67 ± 1.92	2.91 ± 0.25
180 projections	2.12 ± 0.90	2.95 ± 0.26
360 projections	1.45 ± 0.70	2.95 ± 0.27

Table 2: Noise and spatial resolution values for Octopus CT reconstructions of Shepp-Logan images. 10% MTF values is in line pairs per mm.

Shepp-Logan	Noise(HU)	10% MTF
72 projections	10.03 ± 4.55	4.16 ± 1.46
180 projections	3.25 ± 1.61	4.74 ± 1.6
360 projections	1.33 ± 0.51	4.74 ± 1.6

results in a rippling pattern in the images.

Tables 1 and 2 shows the measured noise and spatial resolution values for mART and Octopus CT reconstructions respectively, where values were determined over 10 neighbouring slices in the 3D reconstructed volume. In both case, with an increase in the number of projections used during reconstruction the noise in the image decreases, reflected in the images shown in Figure 2. While there is no statistical difference in the noise between mART and Octopus at 360 projections, at 72 projections the noise in mART images is approximately half of that in Octopus images, seen as the enhanced rippling seen in Figure 2(a), indicating a higher deviation in attenuation across the slice reconstructed using Octopus. This has important clinical implications, as it may be possible to utilise a smaller number of projections, delivering a lower x-ray dose to the patient.

Regardless of the reconstruction method used, the spatial resolution is independent of the number of projections. However, Octopus produces finer edge detail with 10% MTF values of ∼4.7 line pairs per mm, compared to ∼2.9 line pairs per mm for mART.

To assess the performance of the implemented SART algorithm on real data, scans of a cylindrical water phantom was used, where scans were taken using a Medipix 3.0 chip with a Si sensor layer. Selected slices from the reconstructions are shown in Figure 3, with the measured noise and spatial resolution indicated in Tables 3 and 4.

For the mART reconstructed slices of the water phantom, the graininess of the images became less prominent, matching the decreasing noise values. However, the spatial resolution (10% MTF) decreased as the number of projections increased from 72 to 180 and 360 projections. This is reflected in the images determined from 360 projection having a blurrier edge than those of the 180 projections and 72 projections. This can be expected as smoothing can blur edge definition.

Looking at the Octopus reconstructed images using 72 projections (Figure 3(a)), the image is extremely grainy, with a noise value of 427.52 ± 136.61HU. It was almost impossible to see any clear details of the image. But the graininess was reduced significantly as the number of projections was increased to 180 and 360, reflected in the measured noise values. However, the smoothness around the phantom edge in the images from 180 and 360 projections was similar

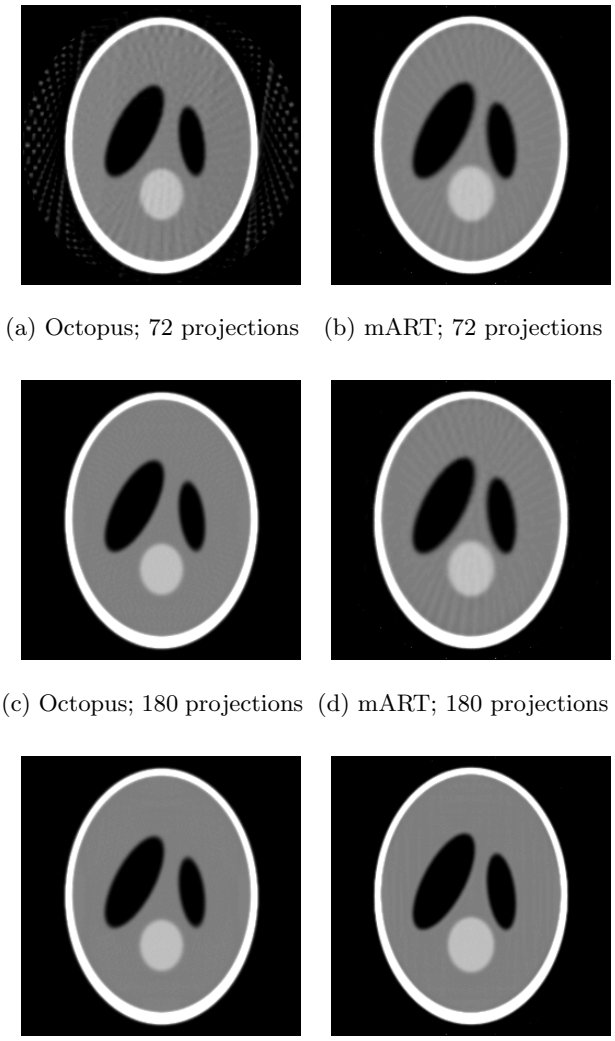

(a) Octopus; 72 projections (b) mART; 72 projections

(c) Octopus; 180 projections (d) mART; 180 projections

(e) Octopus; 360 projections (f) mART; 360 projections

Figure 2: Reconstructed Shepp-Logan Slices.

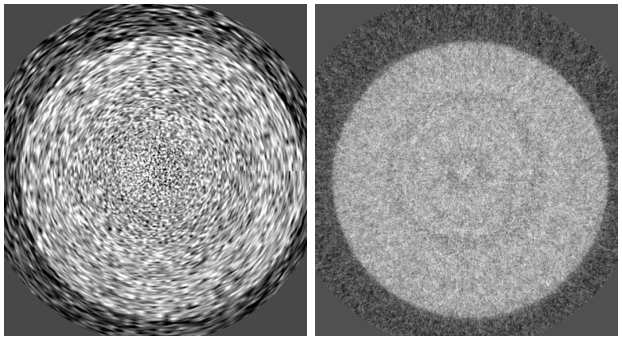

(a) Octopus; 72 projections (b) mART; 72 projections

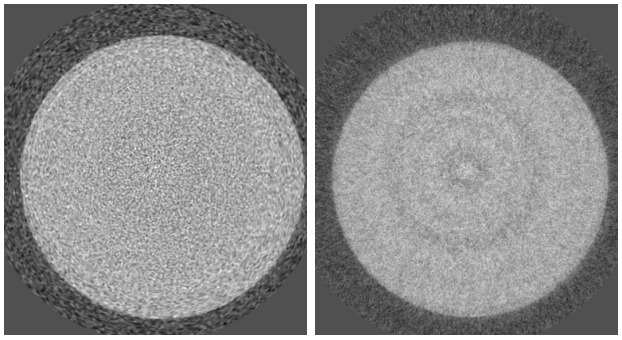

(c) Octopus; 180 projections (d) mART; 180 projections

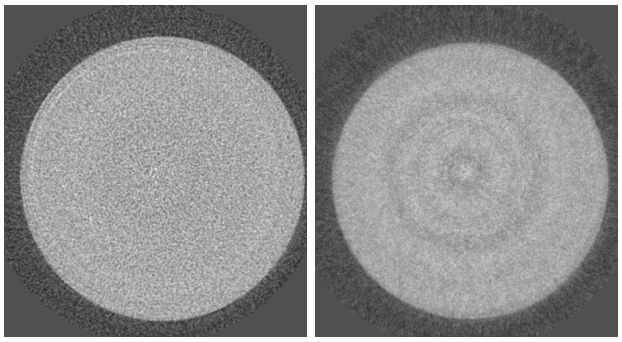

(e) Octopus; 360 projections (f) mART; 360 projections

Figure 3: Reconstructed water phantom Slices.

to each other, with a 10%MTF value of ∼2.4 line pairs per mm.

In general mART will produce images that are less grainy than Octopus, but edges of features may not be as well defined. However if a lower number of projections is to become standard within clinical and pre-clinical applications, to decrease x-ray dosage, mART will produce far superior images.

Figure 4 shows reconstructed slices of an atheroma using both Octopus CT (left) and mART (right), scanned with a CdTe detector at 720 projections. The images shown are scaled to CT numbers. The atheroma sample is located toward the bottom left with a calcified feature indicated with the bright section (HU∼2500). The surrounding capillaries are of air, water and various concentrations of gold and calcium chloride. The Octopus reconstructed image appears to be more grainy than the mART reconstructed image, which is in agreement with values from the quality analysis of the Shepp-Logan and water phantoms above. However, even

Table 3: Noise and spatial resolution values for mART reconstructions of a cylindrical water phantom. 10% MTF values is in line pairs per mm.

Water Phantom	Noise(HU)	10% MTF
72 projections	211.43 ± 85.37	2.92 ± 0.23
180 projections	124.38 ± 39.97	2.72 ± 0.16
360 projections	98.83 ± 35.63	2.65 ± 0.12

Table 4: Noise and spatial resolution values for Octopus CT reconstructions of a cylindrical water phantom. 10% MTF values is in line pairs per mm.

Water phantom	Noise(HU)	10% MTF
72 projections	427.52 ± 136.61	0.74 ± 1.40
180 projections	208.48 ± 97.12	2.42± 0.11
360 projections	151.55± 82.89	2.44 ± 0.08

though the mART reconstructed image appeared smoother and less grainy, it had a more blurry edge compared to the Octopus reconstructed image. This agrees with the differing values of spatial resolution that we obtained earlier, showing that mART reconstructed images have lower spatial resolution than Octopus reconstructed images, albeit slightly.

5. CONCLUSIONS AND FUTURE WORK

The results shown in the previous sections demonstrate that the current application mART produces images of superior quality to Octopus CT for a smaller number of projections. This means that the first milestone in developing a reconstruction algorithm for spectral CT data is complete. The SART algorithm adopted within mART is a flexible algorithm which will allow for rapid extensions based on the nature of spectral CT.

There are three primary tasks which will form the bulk of future research. The first is compressed sensing which will allow reconstructions of higher quality, and hence, lower dose scans. The second is spectral reconstruction which will reconstruct all energy bins simultaneously to exploit the similarities between energy bins. Lastly, is material reconstruction which will fuse the reconstruction algorithm together with a material decomposition algorithm, also in current development. Compressed sensing is an alternative method of solving algebraic linear equations. In our case, this is the ART model from equation (1). The main idea is to incorpo-

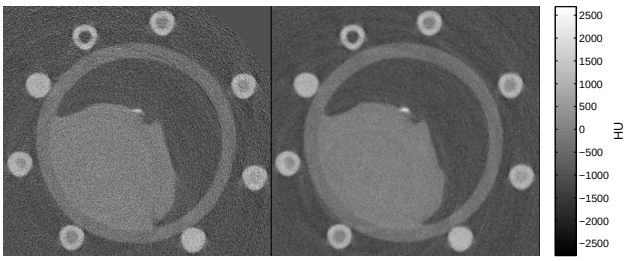

Figure 4: Reconstructed slice of atheroma. Image on left is reconstructed using Octopus CT, whereas image on right is reconstructed using mART. Both images are scaled to HU units.

rate known constraints into the problem. These constraints reduce the number of samples required to reconstruct the original signal. Therefore, reconstruction will require a significantly lower dose.

Spectral reconstruction is when all energy bins are reconstructed simultaneously. This is to exploit the similarities between energy bins such as the geometrical information which is identical between each. If processed correctly, every energy bin should be able to contribute to the spatial resolution of each other and improve image quality. In turn, this should reduce dose requirements further.

Material reconstruction is the fusion of material decomposition and reconstruction. This is possible because the nature of the models for algebraic reconstruction and material decomposition are similar in nature.

The benefit of such a fusion would be two-fold. Firstly, decomposed data has nicer properties such as sparcity (most of the volume would be empty for most target materials) which could be exploited early on. Secondly, a single united algorithm should perform faster than two sequential algorithms.

The potential of spectral CT is vast, and still mostly unexplored. It is our hope that this initial work will contribute greatly to future CT technology.

6. REFERENCES

[1] G. T. Herman. *Fundamentals of computerized tomography: Image reconstruction from projection*, volume 2nd edition. Springer Berlin / Heidelberg, 2009.

[2] *Octopus CT Manual 8.2*. inCT.

[3] T. F. Budinger and G. T. Gullberg. Three-dimensional reconstruction in nuclear medicine by iterative least-squares and Fourier transform techniques. Technical Report LBL–2146, California Univ., Berkeley (USA). Lawrence Berkeley Lab., January 1974.

[4] J. Radon. ÃIJber die bestimmung von funktionen durch ihre integralwerte lÃd'ngs gewisser mannigfaltigkeiten. *Akad. Wiss.*, 69:262–277, 1917.

[5] R. T. H. Bates and T. M. Peters. Towards improvements in tomography. *N. Z. J. Sci.*, 14:883–896, 1971.

[6] G. Hounsfield. Computerized transverse axial scanning (tomography): Part 1. description of system. *Brit. J. Radiol.*, 46:1016–1022, 1973.

[7] S. Kaczmarz. AngenÃd'herte auflÃűsung von systemen linearer gleichungen. *Bulletin International de l'AcadÃl'mie Polonaise des Sciences et des Lettres. Classe des Sciences MathÃl'matiques et Naturelles. SÃl'rie A, Sciences MathÃl'matiques*, 35:355–357, 1937.

[8] P. Gilbert. Iterative methods for the three-dimensional reconstruction of an object from projections. *J. Theor. Biol.*, 36(1):105 – 117, 1972.

[9] A. Andersen and A. Kak. Simultaneous Algebraic Reconstruction Technique (SART): A superior implementation of the ART algorithm. *Ultrasonic Imaging*, 6(1):81 – 94, 1984.

[10] R. Gordon, R. Bender, and G. T. Herman. Algebraic Reconstruction Techniques (ART) for three-dimensional electron microscopy and X-ray photography. *J. Theor. Biol.*, 29(3):471 – 481, 1970.

[11] G.-H. Chen, J. Tang, and S. Leng. Prior image constrained compressed sensing (PICCS): A method to accurately reconstruct dynamic CT images from highly undersampled projection data sets. *Med. Phys.*, 35(2):660–663, 2008.

[12] H. Guan and R. Gordon. Computed tomography using algebraic reconstruction techniques (ARTs) with different projection access schemes: a comparison study under practical situations. *Physics in Medicine and Biology*, 41(9):1727, 1996.

[13] *Standard Test Method for Measurement of Computed Tomography (CT) System Performance*. ASTM International Standard E1695-95 (Reapproved 2006).